Tailoring the Ultrafast Dephasing of Quasiparticles in Metallic Photonic Crystals

T. Zentgraf,[1] A. Christ,[1] J. Kuhl,[1] and H. Giessen[2]
[1]*Max-Planck-Institut für Festkörperforschung, 70569 Stuttgart, Germany*
[2]*Institute of Applied Physics, University of Bonn, 53115 Bonn, Germany*
(Received 30 July 2004; published 7 December 2004)

The ultrafast dephasing of waveguide-plasmon polaritons in metallic photonic crystal slabs is investigated in the femtosecond regime by second-order nonlinear autocorrelation. We find a drastic modification of the dephasing rates due to interaction between localized particle plasmons and optical waveguide modes and subsequent modification of the photonic density of states. In the strong coupling regime our measurements give clear evidence for the appearance of ultrafast polaritonic beat phenomena. All experimental results agree well with theoretical simulations based on a coupled damped harmonic oscillator model.

DOI: 10.1103/PhysRevLett.93.243901 PACS numbers: 42.70.Qs, 61.46.+w, 73.20.Mf, 78.47.+p

Tailoring the optical density of states by using photonic crystal structures is one of the key issues in current compound materials research. The original proposal by Yablonovitch *et al.* suggested a reduction of the spontaneous emission of two-level systems embedded in three-dimensional photonic crystals [1]. In addition to semiconductor or molecular excitations [2], particle plasmon excitations, which are coherent collective electron oscillations within a small metal nanostructure, are excellent candidates for demonstrating this effect. Advantageously, particle plasmons couple extremely well to the light modes of the vacuum, and radiative decay is the dominant dephasing process [3]. Therefore, a photonic crystal made of gold nanostructures would be a well suited model system.

Our current investigations on this novel phenomenon are based on two-dimensional (2D) photonic crystal slabs, combining metallic nanostructures with dielectric waveguides. Such structures, which have been manufactured recently [4], support simultaneous electronic and photonic resonances in the same energy range. By appropriate structuring of the sample (see Fig. 1), the interaction of the resonances can be influenced systematically. In this case, a new quasiparticle [waveguide-plasmon polariton (WPP)] emerges due to strong coupling between the waveguide modes and the particle plasmons [5]. The formation of the WPP and therefore the changed dispersion relation [6] results in a modified density of states within the compound system. Especially in situations where the dephasing mechanisms are dominated by radiative processes, the WPP dispersion has major influence on the lifetime of the coherent excitations, and therefore on the dephasing time T_2. Lengthening the T_2 time of particle plasmons is especially useful for surface enhanced Raman scattering applications, where the electric-field enhancement is directly proportional to T_2 [7]. The time constant for the dephasing of the particle plasmon is given by $T_2^{-1} = T_1^{-1}/2 + T_2^{*-1}$, where T_1 describes the inelastic and T_2^* the elastic phase-loss processes. The inelastic decay of the plasmon population occurs by transfer of energy into electron-hole pairs (nonradiative) and reemission of photons (radiative), the latter being the main dephasing channel for large particles [3,8].

Various methods have been proposed for measuring the dephasing time of metal nanoparticles [7,9–11]. In this Letter, we investigate the ultrafast dephasing time T_2 of WPPs in a 2D metallic photonic crystal structure with a nonlinear autocorrelation technique in the time domain. The influence of inhomogeneous broadening of the resonances is neglected in our discussion. Hence, all obtained T_2 times in this Letter can be understood as a lower limit. We extract T_2 for various photonic crystal periods by fitting the obtained autocorrelation functions with an oscillator model. If more than one branch of the polariton is excited by a coherent laser field, ultrafast polariton beats occur, similar to Rabi oscillations in semiconductor quantum-well microcavities [12].

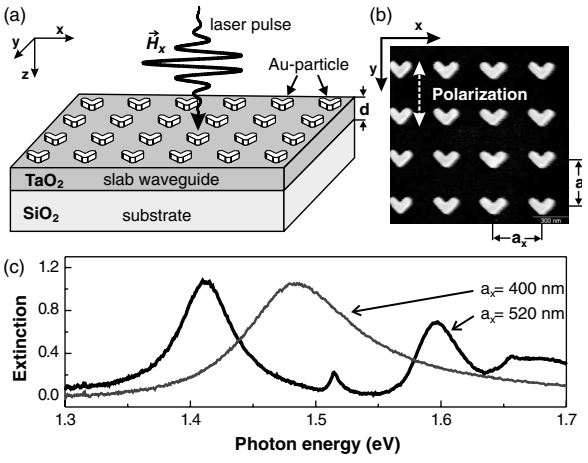

FIG. 1. (a) Sketch of sample geometry with a 100-nm-thick TaO_2-slab waveguide, (b) scanning electron microscope picture of the noncentrosymmetric gold nanoparticle array with a period of $a_x = a_y = 400$ nm, and (c) measured extinction [$-\ln(T)$, T: transmission] spectra for the particle period a_x = 400 and 520 nm.

Electron beam lithography was used to prepare 2D gold nanoparticle arrays on top of a 100-nm-thick tantalum-dioxide (TaO_2) waveguide layer on a quartz substrate. The particles had a noncentrosymmetric L shape to optimize the efficiency of second harmonic generation (SHG) [10]. All metal nanoparticles had the same length (150 nm) and width (75 nm) of the arms with a height of 21 nm. They were arranged in rectangular arrays with a constant periodicity of $a_y = 400$ nm along the y axis. The periodicity a_x along the x axis was changed in steps of 10 nm from 400 to 520 nm (see Fig. 1).

In order to study the dynamics of the WPP, we used a fs time-resolved second-order interferometric autocorrelation technique [13] which is usually applied for ultrashort laser pulse characterization. A short laser pulse was split in a stabilized Michelson interferometer into two equal-intensity pulses with an adjustable time delay τ and subsequently focused onto the sample [Fig. 2(a)]. The second-order autocorrelation function (ACF) for the laser pulse is obtained by measuring the frequency-doubled light. As shown in [10], the ACF contains information about the dephasing time of the plasmon in the nanoparticles.

The local electric field of the particle plasmon can be modeled by a damped harmonic oscillator as described in [13]. In contrast to an undisturbed particle plasmon, the WPP spectrally splits into three polariton branches [5], with each branch j having a specific dephasing time $T_2^{(j)}$. The resonance frequencies ω_j were taken from the extinction spectra of the metallic photonic crystal. Then the plasmon field $E_p(t)$ is proportional to

$$E_p(t) \propto \int_{-\infty}^{t} \sum_j \frac{A_j}{\omega_j} K(t') e^{-\gamma_j (t-t')} \sin[\omega_j (t-t')] dt', \quad (1)$$

where $K(t')$ denotes the driving force, A_j the oscillator strength, and $\gamma_j = 1/T_2^{(j)}$ the damping of the resonance ω_j. $K(t)$ is given by the coherent sum of the two laser pulse fields $E_{\text{light}}(t) + E_{\text{light}}(t+\tau)$ from the interferometer. The theoretical second-order ACF can be obtained by taking the fourth power of the absolute value of $E_p(t)$ for each τ and integrating over time. The temporal dynamics of the WPP were determined by fitting the experimentally obtained ACF with Eq. (1), using A_j and γ_j as fit parameters. This is a quite simplistic approach. Ideally, the theoretical model should include the coupling between the plasmon, the waveguide mode, and the light continuum, giving rise to Fano-type resonances [14].

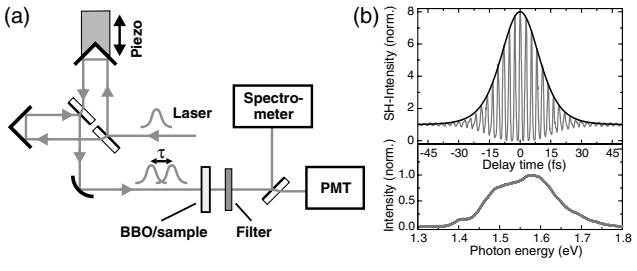

FIG. 2. (a) Experimental setup for the interferometric autocorrelation measurement with a stabilized Michelson interferometer. (b) A second-order autocorrelation function with the BBO crystal (top) and the optical spectrum (bottom) of the laser pulse with $\tau_p = 13$ fs.

A Kerr-lens mode-locked Ti:sapphire laser with a pulse length of about 13 fs and a center wavelength of 810 nm (1.53 eV) was used as a light source. Experimentally, the temporal shape of the laser pulse was determined in the first step. We measured the ACF of the laser in a nonlinear medium using a 20-μm-thick beta barium borate (BBO) crystal, which had a quasi-instantaneous response to the laser pulse [Fig. 2(b)]. In the second step, the BBO crystal was replaced by our metallic photonic crystal structure. The ACF as well as the laser pulse extinction and the SH spectra were measured at several photonic crystal periods a_x. A focused excitation with a numerical aperture of NA < 0.05 was used. The polarization of the laser pulse was set parallel to the y axis (TE polarization), and a_y was fixed at 400 nm in all measurements. This caused the TM waveguide mode (at 2.11 eV, propagating in the y direction) to be far away from the particle plasmon resonance, implying a negligible influence [15]. Figure 3(a) shows the obtained ACF for three selected periods a_x. For $a_x = 400$ nm, the energy of the quasiguided TE mode (1.91 eV) is far away from the plasmon resonance. In this case, an undisturbed particle plasmon can be observed at an energy of 1.48 eV [Fig. 4(a)]. Because of the finite dephasing time of the plasmon, we observed a broadening of the ACF when compared with the BBO crystal (Fig. 3). By fitting the measured ACF with the oscillator model described above, the best agreement appears when assuming a single oscillator with $T_2 = 12$ fs. This value is in good accordance with measurements of the plasmon dephasing in gold nanoparticles by Lamprecht *et al.* [13]. When changing a_x to higher values, the TE mode of the TaO_2 slab moves to lower energies and leads to an increased coupling with the plasmon resonance. Because of the numerical aperture of the laser beam on the sample, both the symmetric and antisymmetric waveguide modes are excited and their interaction with the particle plasmon leads to the formation of three polariton branches [5]. For $a_x = 490$ nm, the two upper polariton branches become visible in the laser extinction spectra [Fig. 4(b)] at energies of 1.65 and 1.58 eV, respectively. The plasmonlike resonance is shifted to lower energies, and the spectral linewidth decreases due to the coupling with the quasiguided TE modes. The measured ACF shows an obvious modulation which is caused by the interference of the polariton branches and is thus a signature of polariton beats. The beating also leads to a modification of the SH spectrum, establishing new frequency components [Fig. 4(b)]. The

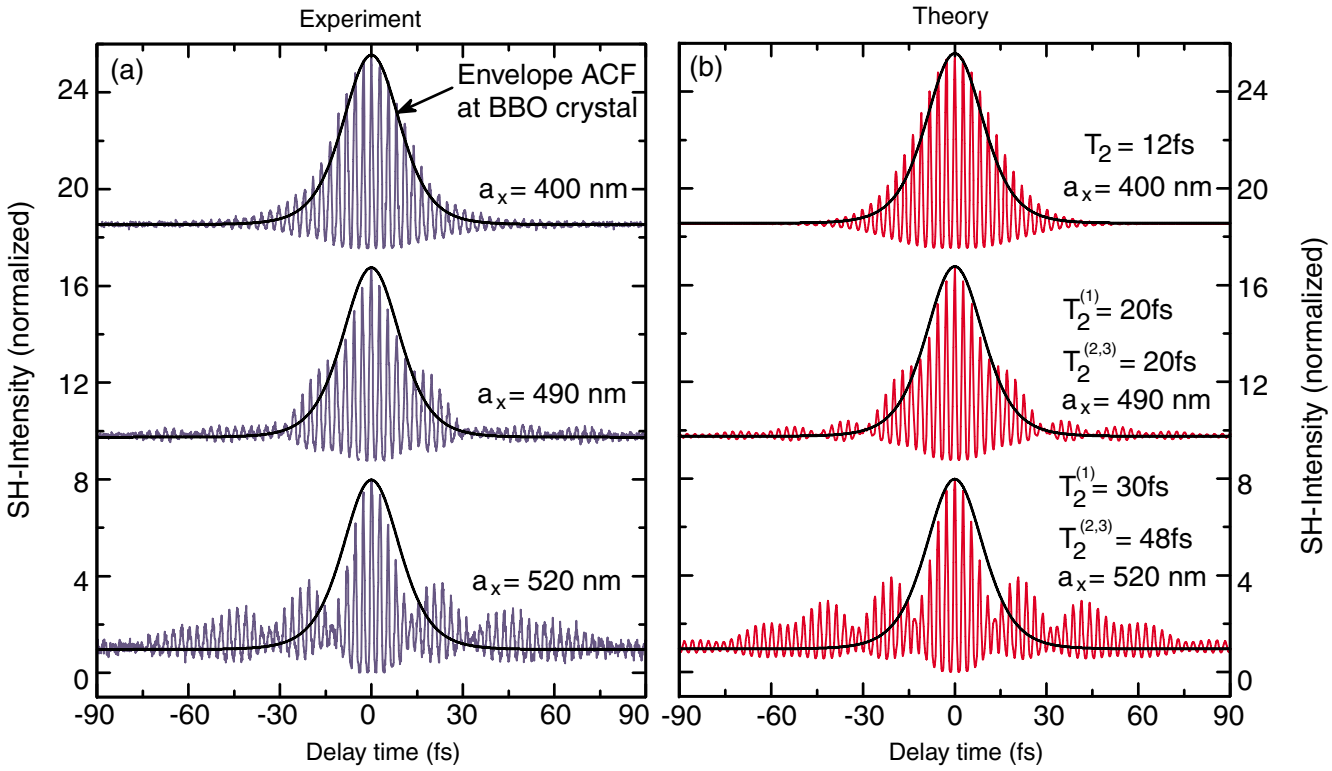

FIG. 3 (color online). (a) Measured second-order interferometric autocorrelation functions for the laser pulse interacting with the nanoparticle fields for three different grating periods a_x of the nanoparticle arrays, and (b) fitted ACFs with the obtained dephasing time T_2 of the polariton branches. The individual ACFs are shifted upwards for clarity in each panel. For comparison, the envelope of the ACF for the laser pulse using the BBO crystal is shown.

best fit for the ACF was found for $T_2^{(1)} = 20$ fs for the lower polariton branch and $T_2^{(2,3)} = 50$ fs for the middle and upper polariton branches. Spatial electric-field simulations show that at energies between the polariton branches the electric field is avoiding the metal nanoparticles [6], which leads to a reduced photonic density of states in this energy region. Therefore, an increased dephasing time of the coupled system can be detected. The even longer dephasing times for the middle and upper polariton branches are caused by their dominantly waveguidelike nature [5,6]. The Fourier transform of the simulated ACF is shown as a theoretical SH spectrum [11] in Fig. 4(e). The experimental and theoretical peak positions and peak widths agree reasonably well.

Increasing the photonic crystal period further to $a_x =$ 520 nm leads to a stronger coupling between the plasmon and the waveguide modes [Fig. 4(c)]. The polariton splitting between the lower and upper branches reaches approximately 200 meV. With this splitting of the polariton branches, we expect a quantum beat period of 21 fs. The ACF is obviously broadened and shows strong modulations of the wings [Fig. 3(a)]. Using our model, the best agreement with the measured ACF was obtained with $T_2^{(1)} = 30$ fs for the lower polariton branch and $T_2^{(2,3)} =$ 48 fs for the middle and upper polariton branches. The interference of the polariton branches leads to nearly fully modulated ultrafast polariton beats with a beat period of approximately 22 fs. This beating should also be visible as a strong modulation of the SHG spectra in the frequency domain. The measured SHG spectrum for this period is shown in Fig. 4(c). Two peaks appear at 3.01 and 3.17 eV at twice the energy of the middle and upper polariton branches. The middle peak at 3.1 eV is interpreted as the sum frequency generation term of the middle and upper polariton branches. The fact that the SHG component of the lower polariton branch does not appear is due to the small laser power at 1.4 eV [see Fig. 4(a), dashed line]. The Fourier transformed spectrum of the calculated ACF [Fig. 4(f)] also shows three peaks. The positions and the widths of the peaks agree very well with the measured ones. The appearance of the WPP leads to a drastically prolonged dephasing time when compared with the undisturbed plasmon dephasing time of $T_2 =$ 12 fs. As shown in [5], it is possible to tailor the interaction between the plasmon and the light field by detuning the waveguide mode versus the particle plasmon resonance. This coupling leads to a modification of the density of states for the WPP. In the case of strong coupling, the new density of states of the polaritonic system causes a changed radiative relaxation rate. This allows tailoring the T_2 time of the WPP in our metallic photonic crystal structure.

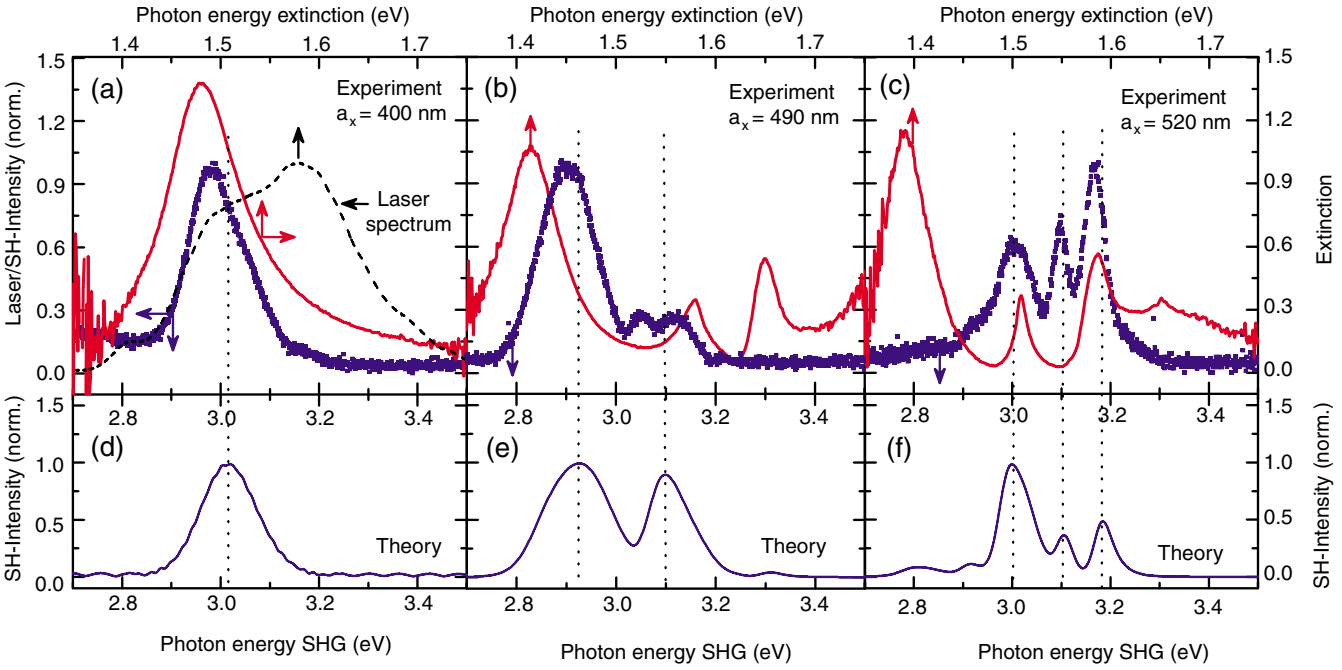

FIG. 4 (color online). (a)–(c) Extinction spectra (solid red line) and corresponding SH spectra (dotted blue line) of the laser pulse measured at the nanoparticle fields. (d)–(f) Calculated SH spectra obtained by Fourier transformation of the fitted ACF. Vertical dotted lines mark the position of maxima in the calculated SH spectrum. In (a) the used laser spectrum is superimposed for clarification.

In conclusion, time-resolved nonlinear measurements have shown a prolonged dephasing time of waveguide-plasmon polaritons in metallic photonic crystals when compared to an undisturbed particle plasmon. The experimental results clearly demonstrate that it is possible to tailor the dephasing of the coherent excitation in metallic photonic crystals by tuning the coupling strength between the electronic and photonic resonances. Good agreement between the measured and calculated autocorrelation functions show that the damped harmonic oscillator model can be used to fit the experimental results with high accuracy. Additionally, if more than one polariton branch is excited, the large polariton splitting between the individual branches leads to ultrafast polariton beats in the second harmonic signal. The possibility to influence the plasmon dephasing time makes such structures attractive for future plasmonic nanodevices.

The authors thank K. von Klitzing for continuous support, U. Waizmann for technical assistance, M. Klein, S. Linden, and M. Wegener for important and valuable suggestions, and K. Schubert for discussions. This work was financially supported by the German Bundesminister für Bildung und Forschung (FKZ 13N8340/1) and the Deutsche Forschungsgemeinschaft (Priority Program SP1113 and FOR557).

[1] E. Yablonovitch, Phys. Rev. Lett. **58**, 2059 (1987).
[2] K. J. Vahala, Nature (London) **424**, 839 (2003).
[3] C. Sönnichsen, T. Franzl, T. Wilk, G. von Plessen, J. Feldmann, O. Wilson, and P. Mulvaney, Phys. Rev. Lett. **88**, 077402 (2002).
[4] S. Linden, J. Kuhl, and H. Giessen, Phys. Rev. Lett. **86**, 4688 (2001).
[5] A. Christ, S. G. Tikhodeev, N. A. Gippius, J. Kuhl, and H. Giessen, Phys. Rev. Lett. **91**, 183901 (2003).
[6] A. Christ, T. Zentgraf, J. Kuhl, S. G. Tikhodeev, N. A. Gippius, and H. Giessen, Phys. Rev. B **70**, 125113 (2004).
[7] T. Klar, M. Perner, S. Grosse, G. von Plessen, W. Spirkl, and J. Feldmann, Phys. Rev. Lett. **80**, 4249 (1998).
[8] M. Meier and A. Wokaun, Opt. Lett. **8**, 581 (1983).
[9] F. Stietz, J. Bosbach, T. Wenzel, T. Vartanyan, A. Goldmann, and F. Träger, Phys. Rev. Lett. **84**, 5644 (2000).
[10] B. Lamprecht, A. Leitner, and F. R. Aussenegg, Appl. Phys. B **68**, 419 (1999).
[11] Y.-H. Liau, A. N. Unterreiner, Q. Chang, and N. F. Scherer, J. Phys. Chem. B **105**, 2135 (2001).
[12] J. D. Berger, O. Lyngnes, H. M. Gibbs, G. Khitrova, T. R. Nelson, E. K. Lindmark, A. V. Kavokin, M. A. Kaliteevski, and V. V. Zapasskii, Phys. Rev. B **54**, 1975 (1996).
[13] B. Lamprecht, J. R. Krenn, A. Leitner, and F. R. Aussenegg, Phys. Rev. Lett. **83**, 4421 (1999).
[14] Some groups have recently modeled metallic biperiodic structures that are slightly different from ours. See, for example, L. Martín-Moreno *et al.*, Phys. Rev. Lett. **86**, 1114 (2001) or K. J. Klein Koerkamp *et al.*, Phys. Rev. Lett. **92**, 183901 (2004).
[15] S. Linden, J. Kuhl, and H. Giessen, Appl. Phys. B **73**, 311 (2001).